25th ABCM International Congress of Mechanical Engineering
October 20-25, 2019, Uberlândia, MG, Brazil

COBEM-2019-1702
CHARACTERIZATION OF UHTC ZrB_2 / SiC COMPOSITE MATERIALS EXPOSED TO HYPERSONIC PLASMA TORCH SIMULATING AEROSPACE APPLICATIONS

Cristian Cley Paterniani Rita
ITA – Instituto Tecnológico de Aeronáutica, Praça Marechal Eduardo Gomes,50 – Vila das Acácias. CEP 12.228-900 – São José dos Campos – SP – Brasil. Fatec – Faculdade de Tecnologia de Pindamonhangaba, Rodovia Vereador Abel Fabricio Dias, 4010 – Água Petra. CEP 12445-010 – Pindamonhangaba –SP – Brasil.
cpaterniani@yahoo.com.br

Felipe de Souza Miranda
ITA – Instituto Tecnológico de Aeronáutica, Praça Marechal Eduardo Gomes,50 – Vila das Acácias. CEP 12.228-900 – São José dos Campos – SP – Brasil
mirannda.fs@gmail.com

Felipe Rocha Caliari
ITA – Instituto Tecnológico de Aeronáutica, Praça Marechal Eduardo Gomes,50 – Vila das Acácias. CEP 12.228-900 – São José dos Campos – SP – Brasil
felipercaliari@yahoo.com.br

Rosa Maria Rocha
IAE – Instituto de Aeronáutica e Espaço – Praça Marechal Eduardo Gomes,50 – Vila das Acácias. CEP 12.228-900 – São José dos Campos – SP – Brasil
rosa.rocha11@gmail.com

Alexei Mikhailovich Essiptchouk
UNESP – Universidade Estadual Paulista – Rodovia Presidente Dutra, Km 137,8 - Eugênio de Melo - CEP 12247-004 - São José dos Campos – SP, Brasil
alexei.essiptchouk@gmail.com

Leonid Ivanovich Charakhovski
LUIKOV – Heat and Mass Transfer Institute, National Academy of Sciences of Belarus, 220072, Minsk, Rep. Belarus
leonidsh.hmti@gmail.com

Gilberto Petraconi Filho
ITA – Instituto Tecnológico de Aeronáutica, Praça Marechal Eduardo Gomes,50 – Vila das Acácias. CEP 12.228-900 – São José dos Campos – SP – Brasil
petrafilho@gmail.com

Abstract. *The successful implementation of hypersonic vehicles and evolution of space capsules used at the atmospheric reentry, relies on the deep understanding of aerothermodynamic load effect on the new class of materials called ultra-high temp ceramic (UHTC). This approach demands experimental data of ablation resistance of UHTC materials under hypersonic regime, which is rarely discussed in the literature. For this reason, the present study aims to investigate the degradation mechanism of ZrB_2-SiC based materials, tested in a plasma wind tunnel, capable of generating a hypersonic plasma jet and simulating the reentry atmosphere conditions. The air plasma jet used to promote the ablative environment has thermal flux of 1.7 MW/m^2, average enthalpy of 18.5 MJ / kg and Mach number 5. The effect of ablative environment at hypersonic flow on the microstructure of ZrB_2-SiC, with different SiC percentage in volume (10, 20 and 30%) were discussed through the results obtained from the XRD, SEM and EDS analysis.*

Keywords: *Plasma Wind Tunnel, UHTC Materials, Plasma Jet, Hypersonic Flow, Hypersonic Plasma Torch*

1. INTRODUCTION

During the process of re-entry into the atmosphere, a manned or unmanned spacecraft at hypersonic speed undergoes a marked deceleration process in relation to the atmosphere. The high kinetic energy of this movement generates intense shock waves and high heat fluxes on the surface of aerospace vehicles (Bletzinger et al., 2005, Kuo et al., 2001). The material used as thermal protection system must be able to withstand environmental conditions and dissipate the flow of heating energy. Ultra-High Temperature (UHTC) ceramics are currently the most widely used materials in Thermal Protection Systems (TPS) because of their superior thermal and ablative properties compared to conventional materials (Fahrenholtz et al., 2014). Some UHTCs used in TPS have adaptive capacity when subjected to intense thermal flow, such as those applied in hypersonic aerospace vehicles or reusable atmospheric reentry vehicles (Schwartz, 2007). This composite material combines essential qualities such as: high melting temperature, oxidation resistant and good chemical inertia (Fahrenholtz, 2014, Parthasarathy et al., 2013). Even in these materials loss of mass and dimensions are expected when subjected to plasma oxidation and ablation processes. These processes involve a series of reaction products, which are dependent on: ambient pressure, plasma jet velocity and temperature, enthalpy, thermal flow, maximum stagnation pressure, material properties and ablation by-products (Kaiser et al., 2008, Parthasarathy et al., 2013).

Although there are many studies related to the oxidation, ablation and general properties of UHTC ZrB_2-SiC, in most cases the tests are performed at low speeds and / or Mach number, making it impossible to analyze the actual application conditions that are proposed for these class of materials. In atmospheric reentry, the vehicle can reach hypersonic velocities (Mach > 4), this condition has particular characteristics as: direct effects of continuous and turbulent flow, and increase of Mach number; these effects become progressively more intense, such as the effects of high temperatures, viscous interaction, thin-shock wave layers and entropy layer (Anderson, 2006, Mungiguerra et al., 2019, Bertin, 1994). If necessary, a system capable of simulating the pressure, hypersonic velocity and plasma / material interaction that occurs during atmospheric reentry. Therefore, the objective of this work is to investigate the ablation and microstructural properties of the ZrB_2-SiC samples, considering the SiC variation in volume (10, 20 and 30%), under ablative conditions generated by the Wind Plasma Tunnel pressure (216 Pa), which is equipped with a thermal plasma torch, with hypersonic plasma jet (Mach 5) and a continuous and turbulent flow (Re ~ 1×10^5). The air plasma jet generates a plasma jet with a thermal flow of 1.7 (MW / m^2) and an average enthalpy of 18.5 (MJ / kg). This system makes it possible to simulate atmospheric reentry conditions and provide facilities to evaluate the ablative, thermal and microstructural properties of thermal protection materials. To investigate the changes in the composite material after the ablative tests, the morphology and chemical composition of the surfaces and cross-sections of each sample were studied by MEV / EDS and the crystalline phases of the materials were identified by XRD, this set of results are discussed and correlated with mass loss, by-product formation due to oxidation mechanisms and ablation rate.

2. MATERIALS AND METHODS

2.1. Preparation of ZrB_2-SiC composites

In this work the ZrB_2 and β-SiC powders were used with raw materials. Coarse powder of ZrB_2 was obtained from the ESK (Elektroschmelzwerk Kempten-Germany) and fine β-SiC powder, BF-12 grade (H.C. Starck-Germany), with equivalent diameter the 0.9 μm and 11.9 μm for SiC and ZrB_2, respectively. The particle size distributions were measured by laser diffraction (Malvern- Mastersizer 2000). The powder mixtures were prepared by planetary milling in isopropanol using a polyethylene container and silicon carbide spheres. The weight ratio of powders to SiC media was about 1:2 and the mixture time was 4 h. Three different composites were prepared with SiC concentration of 10, 20 and 30 vol% (ZS10, ZS20 and ZS30), respectively. The powder mixtures were prepared by planetary grinding in isopropanol using a polyethylene vessel and silicon carbide beads. The weight ratio of powders to the SiC medium was about 1: 2 and the mixing time was 4 h. After drying and sieving, the blends were pressed uniaxially into samples in the cylindrical format 20 mm in diameter and 5 mm thick and then subjected to cold isostatic pressing at 300 MPa. The samples passed through the sintering process, performed at IAE (Institute of Aeronautics and Space) (Juliani et al., 2015).

2.2. Plasma Wind Tunnel

The experimental apparatus, Figure 1 is composed by a stainless-steel vacuum chamber (3 m^3); vacuum system with two stage rotary pumps (160 m^3/h) connected to a booster roots (500 m^3/h); pressure sensors and gas lines (oxygen, nitrogen, argon, hydrogen) with mass flow. Through a programmable controller connected to a valve it is possible to automatically adjust the pumping speed, keeping the constant pressure 216 Pa inside of the vacuum chamber, for small variations in the injected gas flow.

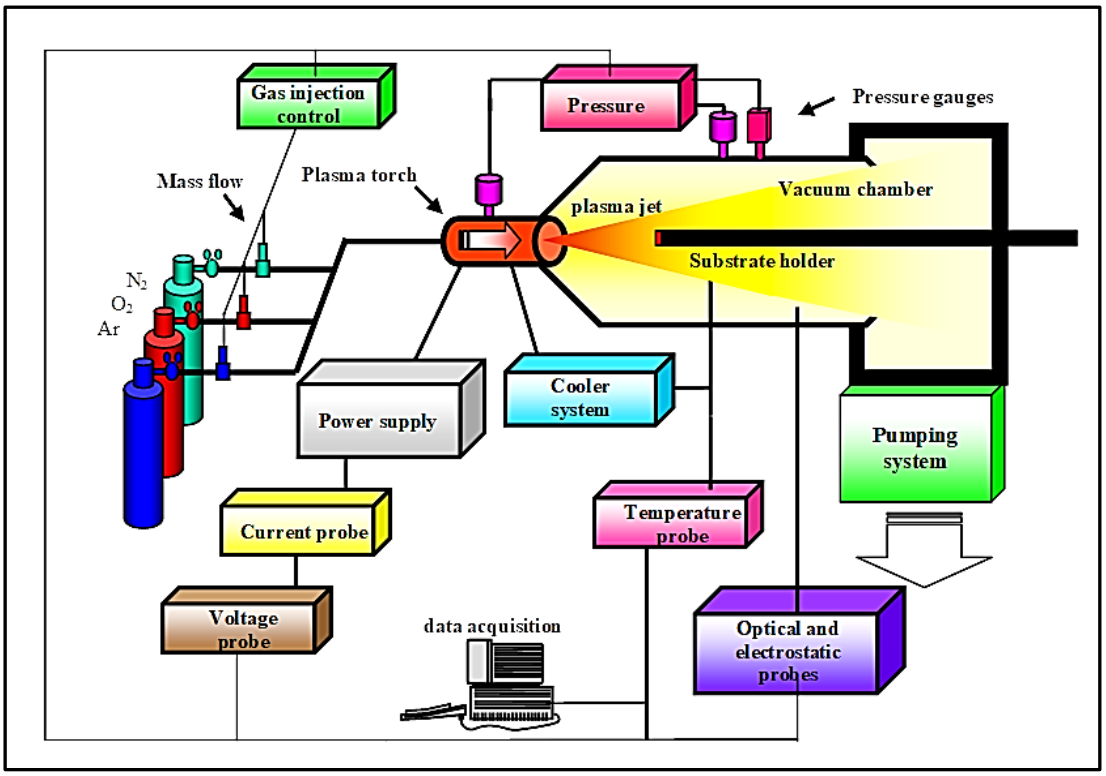

Figure 1. Schematic diagram of the experimental apparatus.

The system has a non-transferred arc plasma torch, which operates with direct current (DC), cooled internally through the forced water circulation. A divergent-convergent nozzle is coupled to the plasma torch, which allows the operation with hypersonic plasma jet (Mach 5). Figure 2 shows the schematic drawing of the plasma torch and sample holder arrangement with a max capacity of 8 samples. The sample holder has freedom rotation (360º), allowing changing the sample for execution of 8 sequential tests.

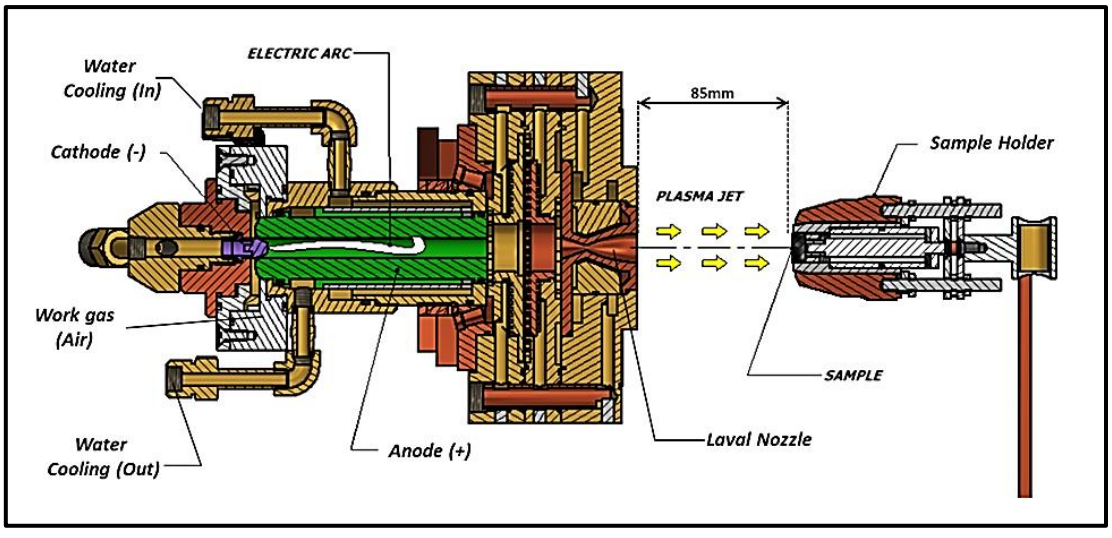

Figure 2. Schematic drawing of the plasma torch and sample holder arrangement.

2.3. Ablation tests

The ablation tests were performed with the air working gas flow rate of 20 l/min. The operating parameters of the plasma torch were fixed at the current and voltage of 110 A and 340 V, respectively. These operational parameters generate a hypersonic plasma jet with thermal flux of 1,7 (MW / m^2) and average enthalpy of 18.5 (MJ / kg). The samples (ZS10, ZS20 and ZS30) were exposed to the plasma jet during 40s, maintained at the fixed stand-off distance of 85 mm.

Measurements of temperatures on sample surfaces were performed using an infrared pyrometer, Pyrofiber Lab. The mass and thickness of each sample were measured before and after the ablation test.

2.4. Oxidation Mechanism

When materials are subjected to the plasma oxidation and ablation processes, occurs the reduction of the dimensions and this process involves a series of reaction products, which are dependent of: environment pressure, plasma jet velocity and temperature, enthalpy, thermal flux, properties of the material used and the ablation by-products (Kaiser, 2007; Parthasarathy, 2013). The understandings of the oxidation mechanism, which may be passive or active, has a fundamental importance when considering applications under hypersonic flow. Under active oxidation mechanism of ZrB_2-SiC composite, the formation of a protective layer of SiO_2 on the surface is aborted forming only volatile gases of B_2O_3, BO_2, B_2O, SiO and CO, resulting in a fast consumption, as shown by the reactions (1-4).

$$ZrB_{2(s)} + \frac{5}{2}\, O_{2(g)} \rightarrow\ ZrO_{2(s)} +\ B_2O_{3(g)} \quad (1)$$

$$ZrB_{2(s)} + 3\, O_{2(g)} \rightarrow\ ZrO_{2(s)} +\ 2BO_{2(g)} \quad (2)$$

$$ZrB_{2(s)} + \frac{3}{2}\, O_{2(g)} \rightarrow\ ZrO_{2(s)} +\ B_2O_{(g)} \quad (3)$$

$$SiC_{(s)} + 2\, SiO_{2(g)} \rightarrow\ 3\, SiO_{(g)} +\ CO_{(g)} \quad (4)$$

The other oxidation mechanism, called "passive", chemical reaction equations (5-7) occurs preferably at lower temperatures and higher partial pressures of oxidant. In this regime the formation of a stable layer of SiO_2 on the surface allows the reduction of the diffusion of oxidants for the UHTC ceramics and consequently also reducing the mass loss rate (Wang, 2017; Zhang, 2008).

$$SiC_{(s)} + \frac{3}{2}\, O_{2(g)} \rightarrow\ SiO_{2(s)} +\ CO_{(g)} \quad (5)$$

$$SiO_{(g)} + O_{2(g)} \rightarrow\ 2\, SiO_{2(l)} \quad (6)$$

$$ZrO_{2(s)} + SiO_{2(l)} \rightarrow\ ZrSiO_{4(s)} \quad (7)$$

Fahrenholtz et al proposed a thermodynamic analysis of ZrB_2–SiC oxidation in air at temperatures about 1500ºC. The main objective of this study was to evaluate the effect of oxidants in a partial pressure on the formation of a SiC-depleted layer, due to active oxidation of SiC. The oxidation of ZrB_2–SiC was analyzed using volatility diagrams for ZrB_2 and SiC, in order to evaluating the formation of SiO (g), SiO_2 (l), ZrO_2 (s), $ZrSiO_4$ and B_2O_3 (g). The formation of $ZrSiO_4$ in ZrB_2-SiC based composite materials submitted to ablation and oxidation processes is desirable, because it is an oxide with higher mechanical and thermal stability, which are desired properties of materials applied in thermal protection systems.

2.5. Microstructural properties

The crystalline structures of the samples were investigated by X-ray diffraction (XRD) using an Empyrean diffractometer (Panalytical), with a step size of 0.013°, with a 2θ interval of 15-100°. The microstructure of the surface and cross-section were observed using a scanning electron microscope (SEM) Vega 3 XMU (Tescan). Cross-sections of the samples were prepared following standard metallographic procedures.

3. RESULTS AND DISCUSSIONS

3.1.Microstructural and morphological analysis

Micrographs of samples ZS10, ZS20 and ZS30, before and after the ablation tests, are presented in Figure 3. The samples before the ablation tests show intact and well-defined regions, as in the micrograph of sample ZS10 Figure 3(A), where it is possible to identify grains of ZrB_2 with an average diameter of 18 microns and the presence of SiC at the grain boundaries. Figure 3(C), referring to sample ZS20, shows an increase in SiC composition at the grain boundaries and the microstructure assumes a bimodal architecture, and a similar behavior is observed for sample ZS30 by Figure 3(E). This fact is also qualitatively observed in the X-ray diffractogram shown in Figure 4 (A). The peaks at 2θ position 25°, 32°,

41°, 58°, 74° corresponding to the hexagonal ZrB_2 crystal structure have constant intensities, whereas the increase of 2θ peaks at 35°, 35°, 60° of samples ZS20 and ZS30 indicate the increase of SiC in the composition.

In the micrographs of Figure 3(B), 3(D) and 3(F) significant changes on the morphology of sample surfaces are observed after ablation tests. The study of the ablative resistance of UHTC exposed to hypersonic plasma jet takes in consideration the enhanced degradation caused by the shock waves and forced convection process, where the energy and air mass transport causes changes and discontinuous effects on the pressure, temperature and density of the plasma jet towards the surface of the samples. A superficial fluidity behavior can be observed on the as-ablated sample surfaces. In the Figure 3(B) e 3(F), one can observe the presence of a colony structure-like of ZrO_2 on the surface of the samples and a bubble formation due to the SiO_2 formation, which became volatile due to the active oxidation mechanism, favoring the chemical reactions (1), (2) and (3) (see section 2.4) that form ZrO_2 fragile layer on the surface of samples and B_2O_3, BO_2 and B_2O in gaseous form. The result of this active oxidation process is the formation of oxide layer with low thermal resistance and highly volatile gaseous materials due to the low SiC composition in the ZS10 samples. The formation of this oxide layer is substantiated by the X-ray diffraction results in Fig. 4(B) where it presents characteristic 2θ peaks for the formation of monoclinic ZrO_2. Fig. 3(D) illustrates the different behavior of ZS20 samples in comparison to sample ZS10. In this case the formation of bubbles is more intense showing that greater oxygen diffusion associated with a highly reactive environment, favoring chemical reactions (5), (6), (7).

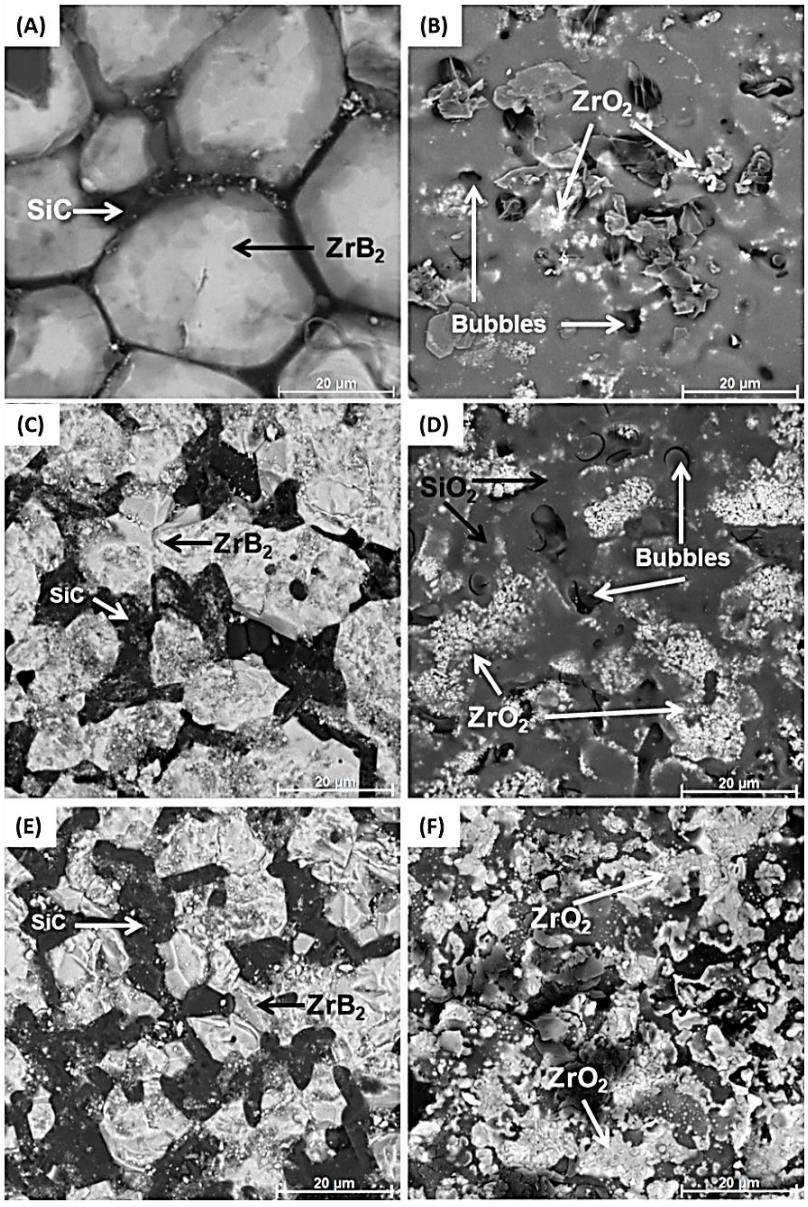

Figure 3. (a), (c), (e) shows samples ZS10, ZS20 and ZS30, respectively, before the ablation tests. The micrographs (b), (d) and (f) present the samples ZS10, ZS20 and ZS30, respectively, after the ablation test.

In the sample ZS10 is shown the result of the active oxidation process, which forms an oxide layer with low ablative resistance and highly volatile gaseous materials due to the low SiC composition. Once the volatilization process take place, the enhanced mass transfer promoted by the hypersonic plasma jet will likely accelerate the ablation process. Figure 3(D) illustrates the different behavior of ZS20 in comparison to ZS10. In this case the formation of bubbles are more intense, as a result of the higher oxygen diffusion associated with a highly reactive environment, favoring by the passive oxidation mechanism. This mechanism occurs preferably at lower temperatures and higher partial pressures of oxidant. This condition enhances the oxidation process from SiC to SiO_2, CO and boron oxidation to B_2O / BO_2 highly volatile, where the remaining composition is based on the ZrO_2 and SiO_2. In this regime after the formation of an oxide layer on the surface, occurs the reduction in the diffusion of oxidants and temperature in deep layers of the sample; which consequently reducing the rate of mass loss

Figure 4 shows X-ray diffractograms, highlighting the formation of oxide phases on the surface of the ZS20, formed by means of the passive oxidation mechanism.

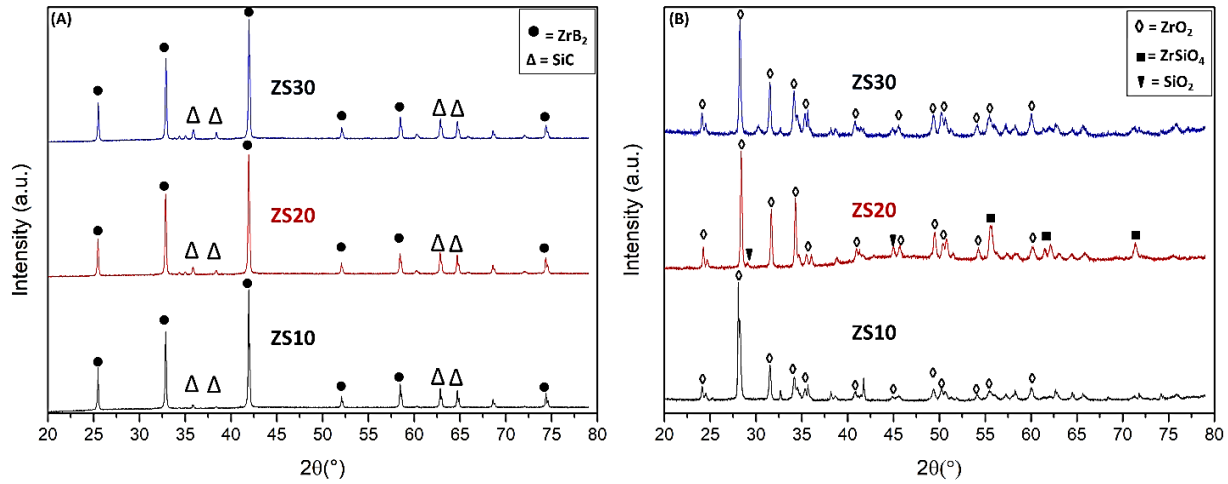

Figure 4. XRD patterns of ZS10, ZS20 and ZS30 samples (A) before ablation test and (B) after ablation test.

The formation of ZrO_2 and a glass layer of SiO_2, which occur during the passive oxidation on the surface of the sample ZS20, can be observed in Figure 4(B). A passivation layer with high thermal resistance is formed, where SiO_2 is located closer to the surface and ZrO_2 in the inner layers, creating a region of interface between layers of high thermal resistance and a specific transition region with formation of zirconium silicate ($ZrSiO_4$), not found in the characterizations of sample ZS10. The formation of $ZrSiO_4$ is due to the oxidation of ZrB2-SiC in a high temperature and high oxygen diffusion environment, forming a ZrO_2-SiO_2 pseudo-binary oxide system. To understand the formation of the zirconium silicate, we can analyze the X-ray diffractogram of Figure 4(A) obtained on the surface of the ZS20 samples when subjected to the ablation test. Under these conditions the presence of crystalline phases of monoclinic ZrO_2 along with the formation of tetragonal SiO_2, as represented in the Figure 4(B). On the other hand, the XRD results does not indicate the presence of carbide phases, and this is because when exposed directly to the air plasma jet with high oxygen concentration, it leads to the formation of SiO_2 and the formation of CO from the oxidation of the SiC.

4.CONCLUSION

The samples of ZrB_2-SiC with variation in SiC concentration in 10, 20 and 30 %vol were submitted to the ablation test using a hypersonic plasma torch (Mach ≅ 5) with thermal flux of 1,7 (MW / m^2) and average enthalpy of 18.5 (MJ / kg) and T = 1930 °C installed in a plasma tunnel. The results of the ablation tests show that the ZS10 and ZS30 samples undergo active oxidation, forming surface based on ZrO_2 and creating regions with mass loss and wear. The results of the ablation tests show that the ZS10 and ZS30 samples undergo to the active oxidation, forming ZrO_2 oxide, which is an unstable and fragile oxide and not withstand the drag force of the hypersonic plasma jet, causing an accentuated loss of mass. For the ZS20, passive oxidation occurred, and the reactions in this mechanism favors the formation of passivation layer of $ZrSiO_4$. The formation of $ZrSiO_4$, which is a stable oxide, promotes a mechanical resistance and consequently low ablation rate. In the opposite way, observed in the ZS10 and ZS30, which had loss of mass, the ZS20 sample obtained a gain of mass. These results can be associated to the variation of SiC composition, demonstrate that there is an ideal proportion of ZrB_2 and SiC, which influence in the mechanisms of formation of these oxides. For this study, the better ablative resistance was obtained in the sample fabricated with 20 %vol SiC.

5. ACKNOWLEDGMENT

This work was supported by AEB, IAE, FAPESP, CNPq and Capes.

6. REFERENCE

Anderson, J. John D. 2006. “hypersonic and high temperature gas dynamics” second edition.

Bertin, J.J. 1994. “Hypersonic aerothermodynamics”, Phys. Today. 627. doi:10.1016/j.energy.2014.09.014.

Bletzinger, P. B.N. Ganguly, D. Van Wie, Garscadden, A. 2005. “Plasmas in high speed aerodynamics”, J. Phys. D. Appl. Phys. 38 . doi:10.1016/S0039-128X(81)90284-1.

Fahrenholtz, W.G. Wuchina, E.J. Lee, W.E. Zhou, Y. 2014. “Ultra-High Temperature Ceramics”, John Wiley & Sons, Inc, Hoboken, NJ, doi:10.1002/9781118700853.

Kaiser, A. Lobert, Telle, M. R. 2008. “Thermal stability of zircon (ZrSiO4)”, J. Eur. Ceram. Soc. (28) 2199–2211. doi:10.1016/j.jeurceramsoc.2007.12.040.

Kuo, S.P. Bivolaru, D. 2001. “Plasma effect on shock waves in a supersonic flow”, Phys. Plasmas. (8) 3258–3264. doi:10.1063/1.1376422.

Mungiguerra,S. Di Martino, G.D. Cecere, A. Savino, R. Silvestroni, L. Vinci, A. Zoli, L. D. Sciti, 2019. Arc-jet wind tunnel characterization of Ultra-High-Temperature Ceramic Matrix Composites, Corros. Sci. doi:10.1016/j.corsci.2018.12.039.

Oliveira Juliani, M. C.D. Rocha, R.M. 2015. “Pressureless Sintering of ZrB2 with β-SiC Addition”, Mater. Sci. Forum. (820) 250–255. doi:10.4028/www.scientific.net/MSF.820.250.

Parthasarathy, T.A. Petry, M.D. Cinibulk, M.K. Mathur, T. Gruber, M.R. 2013. “Thermal and Oxidation Response of UHTC Leading Edge Samples Exposed to Simulated Hypersonic Flight Conditions”, J. Am. Ceram. Soc. (96) 907–915. doi:10.1111/jace.12180.

Schwartz, M. 2007. “Smart Materials”, Birkhäuser Basel, Basel, doi:10.1007/978-3-7643-8227-8.

Wang, S. Li, H. Ren, M. Zuo, Y. Yang, M. Zhang, J. Sun, J. Microstructure and ablation mechanism of C/C-ZrC-SiC composites in a plasma flame, Ceram. Int. 43 (2017) 10661–10667. doi:10.1016/j.ceramint.2017.04.089.

Zhang, X. Hu, P. Han, J. Meng, S. Ablation behavior of ZrB2–SiC ultra high temperature ceramics under simulated atmospheric re-entry conditions, Compos. Sci. Technol. 68 (2008) 1718–1726. doi:10.1016/j.compscitech.2008.02.009.